Article

Triple Langmuir probe for diagnosis of plasma produced by Dielectric Barrier Discharge of parallel plates in atmospheric pressure

Ivan Alves Souza. [1,a)], Joao Freire de Medeiros Neto [1,b)], Antônia Karla Paixão Silveira [1,c)], Thércio Henrique de carvalho Costa [1,d)], Efrain Pantaleon Matamoros [1,e)], Michelle Cequeira Feitor [1,f)] and Rômulo Ribeiro Magalhães Souza [2,g)]

[1)] Federal University of Rio Grande do Norte – Labplasma- UFRN; a) ivanalves@ufrn.edu.br, b) joaonetofm@ufrn.edu.br, c) kkarlapaixao@ufrn.edu.br, d) thercioc@ufrn.edu.br, e) epantaleon@ect.ufrn.br, f) michellemaires@gmail.com.
[2)] Federal University of Piauí- UFPI; g) romulorms@gmail.com

This work aimed to characterize a DBD plasma equipment through optical and electrical measurements, seeking to obtain a greater knowledge of the plasma production process and how it behaves through the adopted parameters, such as frequency and voltage applied between electrodes, at a fixed distance of 1.7 mm. In order to measure them, three different characterization techniques were applied. The first method was the Lissajous figures, a technique quite effective for a complete electrical characterization of DBD equipment. The second technique used was the Optical Emission Spectroscopy, a tool used for the diagnosis of plasma, being it possible to identify the excited species produced in filamentary and diffuse discharge in the plasma. And finally, the triple Langmuir probe technique was used to obtain the electron temperature and electron density. Based on this study, it was possible to identify the equipment efficiency in different regimes. The electron temperature measurement for both systems analyzed were 27.96 eV and 20.69 eV to the filamentary and diffuse regimes, respectively. The density of electrons number to these regimes were 1.09×10^{21} m^{-3} and 1.56×10^{21} m^{-3}.

Keywords: Optical Emission Spectroscopy; Lissajous figures; Triple Langmuir probe.

Preprints (www.preprints.org) | NOT PEER-REVIEWED | Posted: 31 January 2019 doi:10.20944/preprints201901.0323.v1

I. INTRODUCTION

Dielectric Barrier Discharge (DBD) is a method of plasma generation where it is possible to obtain cold plasma at atmospheric pressure. This technique consists in the application of a high potential difference between two electrodes, where at least one of them is coated by a dielectric material, which results in the emergence of plasma microfilaments on the surface of the insulator material used [1]. This technique is already widely used to the superficial modification of polymers, since it transforms hydrophobic polymeric materials into hydrophilic without deteriorating its internal structure [2–4]. It is also used for film deposition [5,6], dental treatments and dermatological treatments [7]. According to Xi-Ming Zhu, when the work gas is the atmospheric air, the main active species generated are the nitrogen molecules (N_2) [8]. There are reports that the use of active N_2 species improves soil properties, enabling their use in agriculture [9], besides it acts as a sterilizer agent eliminating microorganisms [10].

However, it is still necessary to develop studies to master and understand the chemical, physical and existing mechanisms in the DBD plasma and how the adopted parameters have influence and interact in the emergence of the various active species, electrical fields, UV radiation, free radicals, atoms and electronically excited molecules existing in DBD plasma [8].

The pulse frequency and the applied tension are two important parameters of the technique, because they determine the quality of the generated plasma and the energy expenditure [11]. This work aims to measure the electronic temperature of the DBD plasma from parallel plates in atmospheric air to combinations of voltage and frequency parameters, as well as to discover their influences on the active species and high energy electrons present in it and determine how they behave through the working conditions adopted and their operating regimes. Being these determinants conditions, in the treatment of materials, since this knowledge is extremely important both in optimizing the treatments that use this technique as well as offering the minimum risk to the operator and user ([8

II. MATERIALS AND METHODS

For the present study, the DBD reactor was used, Figure 1. In this configuration, the electric field generated by the difference of applied potential between the electrodes ensures that the generated plasma occupies all volume delimited by the area immediately below the anode and the surface of the dielectric covering the lower electrode (cathode).

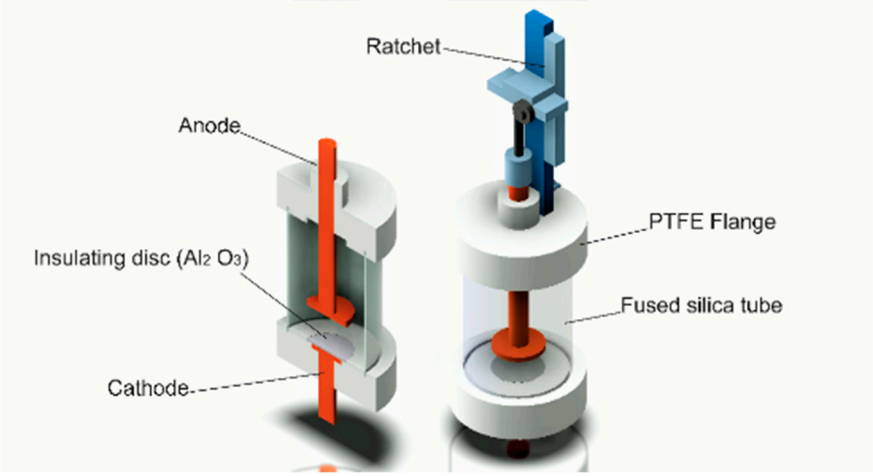

FIG. 1. The project shows the constructive details of the DBD processor Built in the Plasma Materials Processing Laboratory (UFRN).

Preprints (www.preprints.org) | NOT PEER-REVIEWED | Posted: 31 January 2019 doi:10.20944/preprints201901.0323.v1

To generate the plasma, a pulsed high-voltage source was used, with a pulse width of 200 μs, it is capable to vary the applied voltage from 0 to 45 KV and the frequency from 200 Hz to 1.0 kHz. The tests were performed in two parameters, but at a fixed distance of 1.7 mm, the first was performed with 40 kV and the frequency of 740 Hz and the other had a voltage of 34 kV and a frequency of 830 Hz.

The total consumed energy and power of the system were determined from the Lissajous figures built with the aid of an oscilloscope model MSO-X 2002, 2 Agilent channels and a high voltage probe 1000:1. In order to calculate the transported load in each cycle of plasma production, a capacitor of 2.47 nF was placed in series with the output of the reactor. All electrical measurements were performed simultaneously with optical measurements as illustrated n Figure 2.

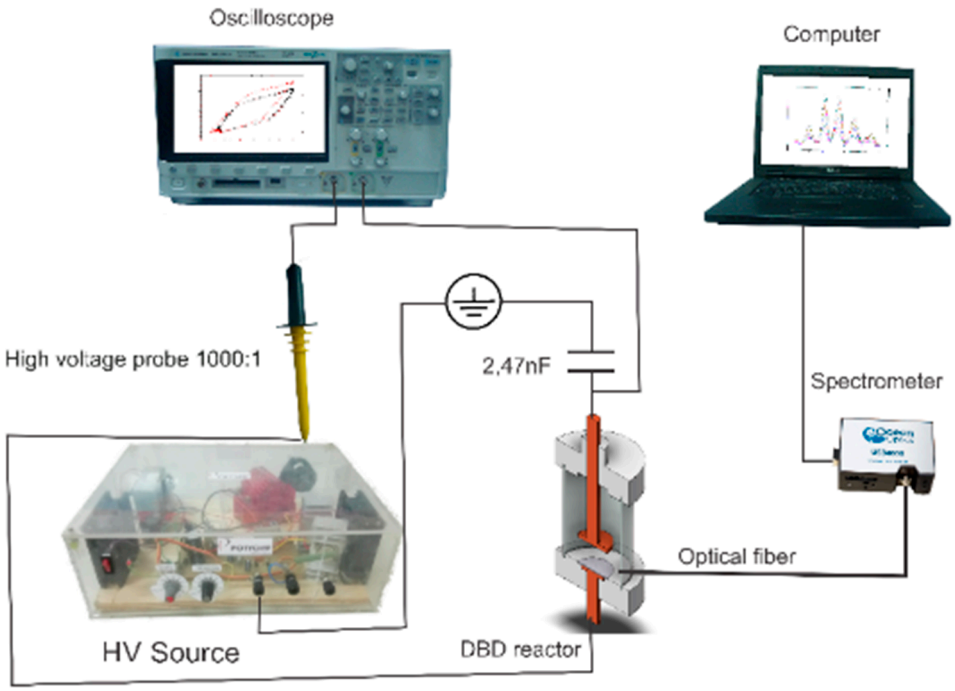

FIG. 2. Scheme of the experimental arrangement of electrical measurements to obtain the Lissajous and optical figures of the excited species in DBD plasma.

The active plasma species were identified with the aid of an optical emission spectrometer model USB4000 UV-VIS, maximum resolution of 1.5 nm. The acquisition of the spectrum was obtained by an optical fiber positioned between the two electrodes at a distance of 1.0 mm from the anode edge, Figure 2, the electron temperature and density were obtained for the both regimens previously mentioned, using the diagram in Figure 3.

Preprints (www.preprints.org) | NOT PEER-REVIEWED | Posted: 31 January 2019 doi:10.20944/preprints201901.0323.v1

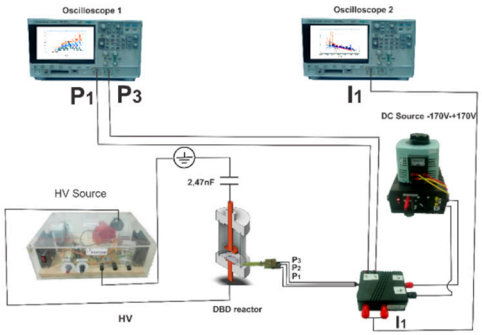

FIG. 3. Experimental arrangement for measurements of electronic temperature and electron number density.

The Langmuir probe was inserted directly into the plasma, as presented Figure 4. P1, P2 and P3 are tungsten electrodes used in the probe that have a diameter of 0.0125 mm, and aim to collect the information from the interior of the plasma. The source provides the necessary potential that serves as reference, a key point in the Langmuir triple probe technique [12], the tension used in this study were 10V and -10 V, potential that is applied between the electrodes P_1 and P_2, P_3 is floating potential. The oscilloscopes 1 and 2 convert the electrical signals into computational data, used to calculate the electronic temperature according to equation 1. Where K is the Boltzmann constant e is the electron charge and V_f is the floating potential measured in P_3.

$$T_e = \left(\frac{e\,(V_{1-3})}{\ln 2}\right) = \left(\frac{e\,(V_1 - V_f)}{\ln 2}\right) \quad (1)$$

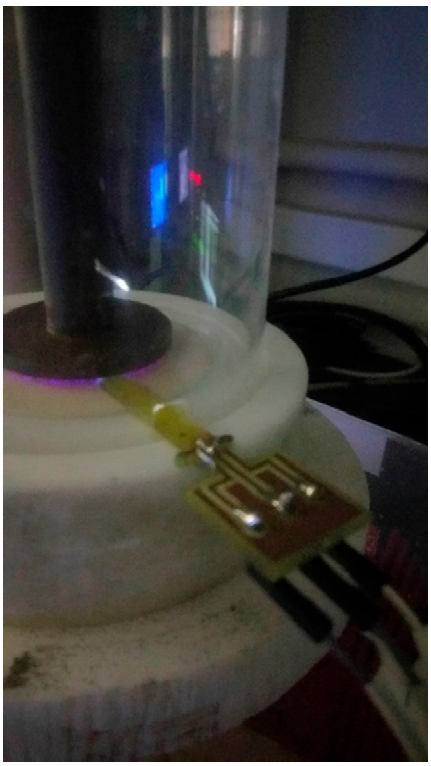

FIG. 4. Triple Langmuir probe positioned for electronic temperature measurement and electron density of plasma DBD atmospheric.

Preprints (www.preprints.org) | NOT PEER-REVIEWED | Posted: 31 January 2019 doi:10.20944/preprints201901.0323.v1

The current I_1 is measured indirectly with the aid of a 45.9 kΩ resistor, which is used to obtain the electron density from Equation 2.

$$n_e = \frac{I_1}{0.61\, e\, A_+ \sqrt{\frac{kT_e}{m_i}}} \frac{exp\left(-\frac{e\,(V1 - V_f)}{kT_e}\right)}{1 - exp\left(-\frac{e\,(V1 - V_f)}{kT_e}\right)} \quad (2)$$

Where A_+ is the area of the transverse section of the tungsten electrode, m_i is the nitrogen ion mass used due to its greater abundance in atmospheric air compared to the other gases.

3. RESULTS AND DISCUSSIONS

This section may be divided by subheadings. It should provide a concise and precise description of the experimental results, their interpretation as well as the experimental conclusions that can be drawn.

A. Optical Emission Spectroscopy (OES)

In the first analysis, it is visible that both regimes have an excitation of the nitrogen molecules of the second positive system [8,13], associated to energy levels $C^3\Pi_u$ and $B^3\Pi_g$ [14] region of electromagnetic emission of UVA. The homogeneity of the plasma in diffuse regime is quite visible, extrapolating even the area delimited by the upper electrode, Figure 5A. This occurs due to a high electric capo reduced as it will be seen later, which does not repeat in the filamentary regime, being it possible to visualize empty spaces between two filament, as presented in Figure 5B. This causes the spectral intensity to be slightly lower due to the lower volume of plasma generated in relation to homogeneous discharge, this justifies the lowest spectral intensity in the filamentary regime presented in Figure 5C.

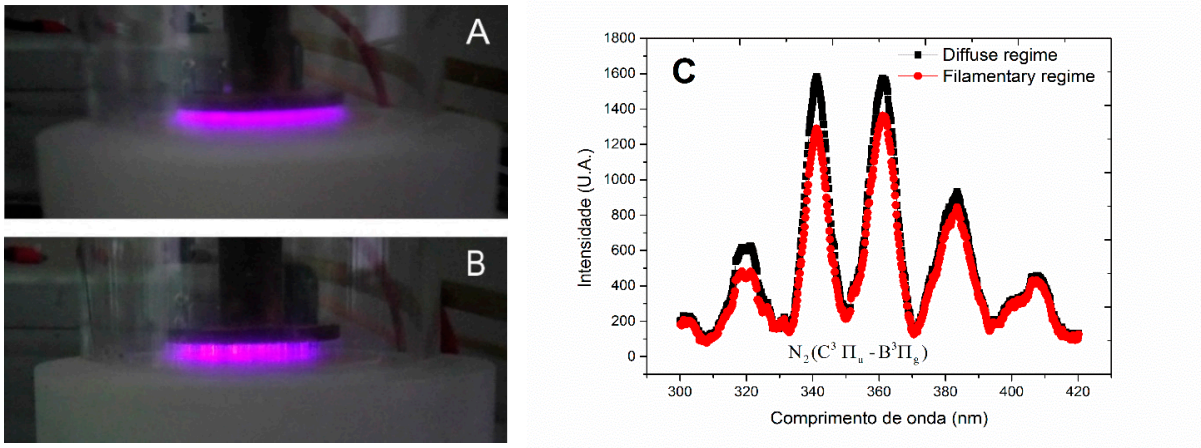

FIG. 5. 5A and 5B, atmospheric DBD plasma generated in the filamentary and diffuse regimes, respectively. In 5C the graphical spectra of the spectral intensities of excited nitrogen.

B. Langmuir Probe

The results obtained through the Langmuir probe technique are shown in Figure 6. It was expected that both curves (red and black) overlap each other, however a displacement was observed.

Preprints (www.preprints.org) | NOT PEER-REVIEWED | Posted: 31 January 2019 doi:10.20944/preprints201901.0323.v1

The mathematical representation attributed to the red and black curve was given by Equation 3 and 4, respectively.

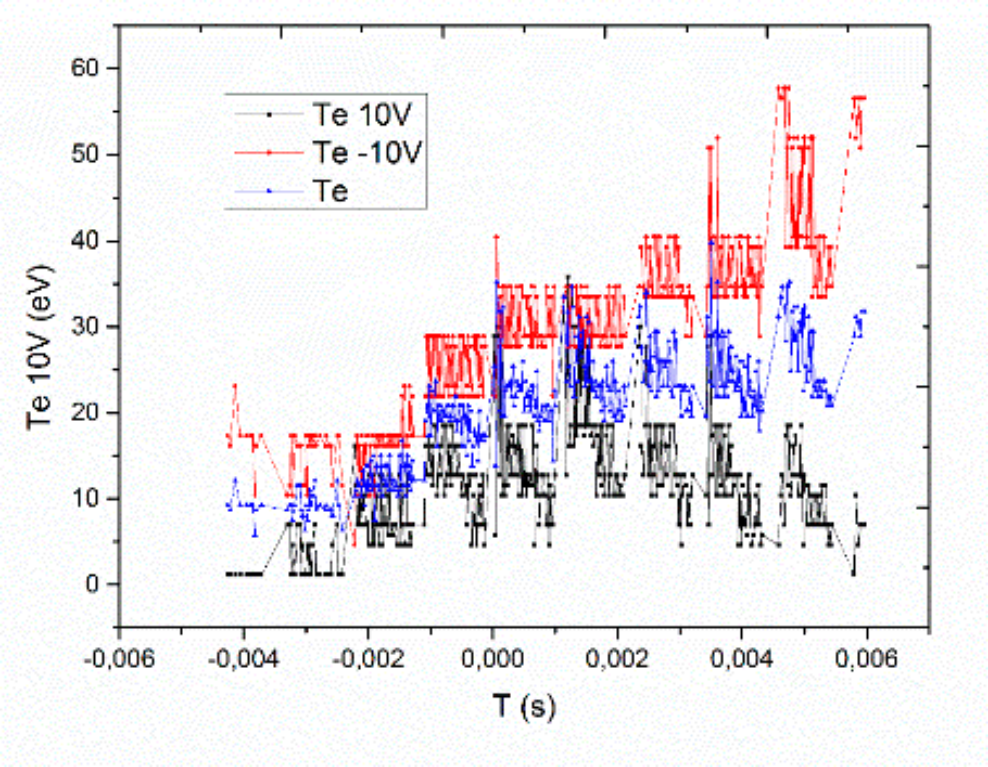

FIG. 6. The red dotted line represents the electronic temperature curve measured from the reference voltage -10V; the black dotted line represents the electronic temperature curve due to the 10V reference voltage and the blue dotted line between the two previous ones.

$$kT_{ev-} = 2e(V_{-v}) \quad (3)$$

$$kT_{e\,v+} = 2e(V_{+v}) \quad (4)$$

The minimum energy for an electron to overcome the potential barrier of the probe is $T_e = 2eV_p/k$ [15], where V_p is the plasma potential. When analyzing the condition of -10 V, tension applied in the probe, it is a fact that the electron current will decrease, once that the negative potential repulse the electrons, therefore only a fraction of them in the plasma will have enough energy to penetrate the potential barrier generated in the probe [16]. Thus, in order to conserve energy, the potential V_{-v} will now be inside the sheath, greater than the potential of the plasma outside the sheath (V_p), that is why the red curve shifts upwards. In the case of the 10V potential, the inverse occurs, the increase in the current in the sheath region promotes the increase of the electronic current, thus the potential V_{+v} of Equation 4 will be lower than V_p. To better understand the analysis, the V_{-v} *and* V_{+v} were expressed as a function of V_p, and with this we have:

$$V_{-v} = V_p + V_\alpha \quad (5)$$

$$V_{+v} = V_p - V_\alpha \quad (6)$$

Preprints (www.preprints.org) | NOT PEER-REVIEWED | Posted: 31 January 2019 doi:10.20944/preprints201901.0323.v1

In equations 5 and 6, V_α represents the increase and decrease of the potential value that still unknown in the sheath region. Then, by replacing 5 and 6 in 3 and 4, respectively, and taking the average, the equation representing the blue curve of Figure 6 was obtained.

$$\frac{k(T_{e+v}+T_{e-v})}{2} = k\overline{Te} = \frac{2e(V_p + V_\alpha + V_p - V_\alpha)}{2} \tag{7}$$

$$\overline{Te} = \frac{2eV_p}{k} \tag{8}$$

It is observed that equation 8 has the value of $\overline{Te}$ exactly equal to the value described by Qayyum for the electronic temperature T_e, so it can be affirmed that the blue curve represents the electronic temperature of the DBD plasma of the present study.

The electron number density was obtained from Equation 2, as well as T_e; n_e was measured for the both operating regimes, these data showed an interesting behavior among them. Figure 7 show the time evolution of them graphically represented, 7A and 7B are the values for the diffuse regime and 7C and 7D are associated to the filamentary regimen. The first difference is the electronic temperature that had the lower mean value, comparing the curves A and C.

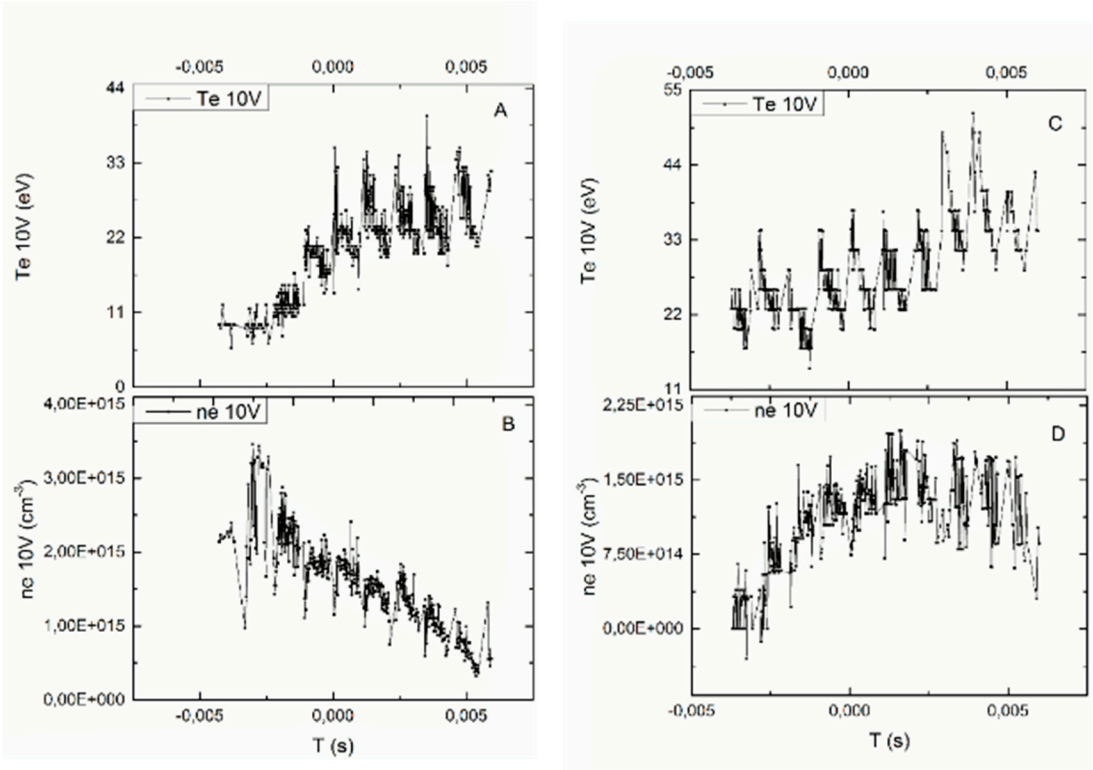

FIG. 7. Graphs as a function of time of electronic temperature and electron density, diffuse regime A and B. Filamentary regime C and D.

In the case of electron number density, the opposite was observed, in the filamentary regime the mean value was lower than in the diffuse regimen. This is evident in the Table 1.

Preprints (www.preprints.org) | NOT PEER-REVIEWED | Posted: 31 January 2019 doi:10.20944/preprints201901.0323.v1

Table 1. Results obtained from the Langmuir triple probe in the two operating regimes

Filamentary		Diffuse	
T_e	27,96 (eV)	T_e	20,69 (eV)
n_e	1,098x10^{15}(cm^{-3})	n_e	1,56 x10^{15}(cm^{-3})
V_p	13,97 (V)	V_p	10,34 (V)

C. Langmuir Probe

In DBD, the plasma always appears in filamentary regimen and, only after the adjustments of the voltage and frequency parameters for a fixed distance, it becomes diffuse. Thus, it can not be attributed a linearity in the electronic temperature with a increase in the applied tension. At 36 kV, T_e, n_e and V_p show the values from Table 1, (left side), while on the right side are the decrease of both T_e and V_p, but n_e had a considerable increase. This occurred due to the transition between regimes, if the plasma potential is seen as a potential density per unit of area, this transition effect is explained coherently.

In the filamentary regime, the plasma is generated due to the accumulation of loads in punctual regions, forming filaments of area much lower than the discharge total area. In the parameter of 40 Kv the entire surface of the dielectric had accumulated the loads evenly, and the processes of excitation, ionization etc.; occurred evenly across the dielectric surface. Therefore, the 6 kV increase is not enough to change the operating regime, however it can not maintain the potential of the plasma at the same time. Consequently, the potential of plasma and the T_e decreases, resulting in a greater amount of electrons emitted inside the discharge region, since the volume of plasma increased, thus allowing a greater distribution of energy to the electrons.

Although the data of OES (Figure 5C) did not revalidate the presence of nitrogen ions in the form N_2^+, possibly due to the small population of species emitting photons in this spectrum band, the limitation of the equipment in observing low-intensity spectrum as is the case N_2^+ generated in DBD of atmospheric air. However, the energy of electrons to generate this species is about 18.50 eV [17], which is within the energy range obtained in the results of this work. In both regimes the average energies of the electrons mediated in the Langmuir probe are more than sufficient to generate excitation of this ion, for the filamentary regimen 27.96 eV and diffuse is 20.69 eV. Thus, it is possible to affirm that the positive nitrogen ions were masked by the high intensity of the excited nitrogen.

Preprints (www.preprints.org) | NOT PEER-REVIEWED | Posted: 31 January 2019 doi:10.20944/preprints201901.0323.v1

Analyzing the plasma from the energy supplied to it, it can relate the energy consumed (power) with the reduced electric field and the electron density, calculated from the energy obtained by the Lissajous figure, Figure 8. This is done using the correlation of Equation 9 [18].

$$n_e = \frac{E_p}{T_e V_{pl}} \tag{9}$$

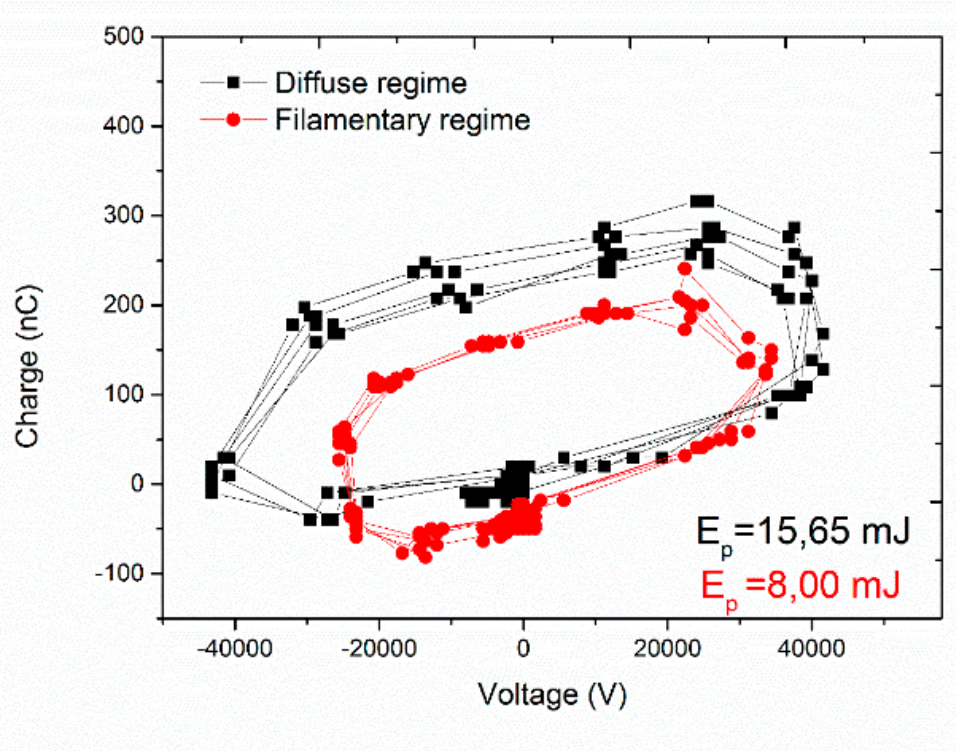

FIG. 8. Graph Charge X Voltage (Figures of Lissajous), formed by 5 consecutive pulses. In the filamentary regime, the frequency is 830 Hz voltage of 34 kV red curve, diffuse regime frequency was order of 720 Hz voltage of 40kV.

These results show inconsistency, because the plasma volume, 2.14 cm^3, is based on the radius from upper electrode anode, and it is clearly seen in Figure 5, that in the filamentary regimen the volume is smaller than that delimited by the electrode, and in the diffuse it extrapolates this region. The density of electrons number is about $1x10^{15}$ cm^3 ([14], value confirmed by the Langmuir probe. Thus, the real plasma volume produced (V_{pl}) for both regimes, calculated by Equation 9, are present in Table 2, so that the results of the Langmuir and Lissajous probe converged. Another important data confirming the results obtained are the values of reduced electric field 700-1000 $V.m^2$ for plasma produced in atmospheric pressure contained in the work of [19], also contained in Table 2.

Table 2. Parameters obtained from the Lissajous figures and the Langmuir probe for the parallel plate reactor of the present work.

Regime	Power (W)	Reduced electric field E/N (Td)	Plasma volume V_{pl} (cm^3)
Diffuse	10,58	1066,7	3,03
Filamentary	6,64	906,7	1,52

This table shows that a small increase in the reduced electric field almost doubled the volume of plasma generated and the power consumed. This occurred due to the better distribution of loads in the work volume that occurred in the transition from the filamentary regime to the diffuse.

In order to better understand the kinetics of DBD plasma production the effective volume of plasma produced V_{pl} was introduced in this paper. Calculated using the equation 9 and the results the Triple Langmuir Probe and Lissajous Figure. This parameter be used in future work to evaluate the energy expenditure, related to the consumed power whit the volume of plasma produced in the reactor.

5. Conclusions

The electronic temperature, power and plasma volume have a direct link with the operation regime. The electronic temperature in the filamentary regime is higher due to the accumulation of punctual loads, however, in the diffuse regime the best distribution of energy optimizes the other factors resulting in practically twice the values of plasma power and volume, besides it increased the intensity of excited nitrogen species. While the reduced electric field has less influence with the operation regime, slightly increasing its value, however a better distribution of loads in the dielectric occurs when the plasma changes regime. The 3 ml of plasma produced from the 10.58 W of power was a good point when shifting it to industrial applications in the near future.

Acknowledgments: The authors would like to thank the team at Laboratório de Processamento de Materiais por Plasma for technical support. And Coordenação de Aperfeiçoamento de Pessoal de Nível Superior - Brasil (CAPES) Funding Support

References

[1] I.A. Souza, 79 (2013).

[2] T. Felix, F.A. Cassini, L.O.B. Benetoli, M.E.R. Dotto, and N.A. Debacher, Appl. Surf. Sci. **403**, 57 (2017).

[3] L. Hu, J. Cheng, Y. Li, J. Liu, J. Zhou, and K. Cen, Appl. Surf. Sci. **413**, 27 (2017).

[4] A. Van Deynse, R. Morent, C. Leys, and N. De Geyter, Appl. Surf. Sci. **419**, 847 (2017).

[5] G. Da Ponte, E. Sardella, F. Fanelli, A. Van Hoeck, R. d'Agostino, S. Paulussen, and P. Favia, Surf. Coatings Technol. **205**, **Suppl**, S525 (2011).

[6] H. Haiyan, G. Qian, Z. Xiwen, and H. Gaorong, Thin Solid Films **In Press,** (2011).

[7] G. Daeschlein, S. Scholz, R. Ahmed, A. Majumdar, T. von Woedtke, H. Haase, M. Niggemeier, E. Kindel, R. Brandenburg, K.D. Weltmann, and M. Jünger, JDDG J. Der Dtsch. Dermatologischen Gesellschaft **10**, 509 (2012).

[8] I.A. de Souza, A.B. do Nascimento Neto, J.C.A. de Queiroz, E.P. Matamoros, T.H. de C. Costa, M.C. Feitor, J.M.L. de Souza, N.T. Camara, and V. da S. Severiano Sobrinho, Mater. Res. **19**, 202 (2016).

[9] N. Lu, J. Lou, C.H. Wang, J. Li, and Y. Wu, Water, Air, Soil Pollut. **225**, 1991 (2014).

[10] M. Amini, M. Ghoranneviss, and S. Abdijadid, Food Chem. (2017).

[11] J.A. López-Fernández, R. Peña-Eguiluz, R. López-Callejas, A. Mercado-Cabrera, B. Jaramillo-Sierra, B. Rodríguez-Mendez, R. Valencia-Alvarado, and A.E. Muñoz-Castro, IEEE Trans. Ind. Electron. **62**, 2215 (2015).

[12] M.U. Farooq, A. Ali, A. Qayyum, M.Y. Naz, Y. Khan, S. Shukrullah, and C.A. Ghaffar, High Energy Chem. **49**, 286 (2015).

[13] I.A. Souza, I.O. Nascimento, A.B. Nascimento Neto, L.A.P. Nascimento, J.M.L. Souza, T.H.C. Costa, and C. Alves Jr, HOLOS **3**, 44 (2015).

[14] A. Zerrouki, H. Motomura, Y. Ikeda, M. Jinno, and M. Yousfi, Plasma Phys. Control. Fusion **58**, 75006 (2016).

[15] A. Qayyum, N. Ahmad, S. Ahmad, F. Deeba, R. Ali, and S. Hussain, Rev. Sci. Instrum. **84**, 123502 (2013).

[16] J.R. Reitz, F.J. Milford, and R.W. Christy, Ed. Campos Ltda 512 (1988).

 doi:10.20944/preprints201901.0323.v1

[17] S.B. Bayram and M. V Freamat, Am. J. Phys. **80**, 664 (2012).

[18] X. Zhang, H. Xiao, X. Hu, and Y. Zhang, IEEE Trans. Plasma Sci. **46**, 563 (2018).

[19] Y. Ju and W. Sun, Prog. Energy Combust. Sci. **48**, 21 (2015).